In-wheel Motor Design for Electric Vehicles

K. Cakir   A. Sabanovic

Sabanci University/Faculty of Engineering and Natural Sciences, Istanbul, Turkey
kazimc@su.sabanciuniv.edu   asif@sabanciuniv.edu

Abstract—**In this work an in-wheel electric motor prototype has been designed for experimental purposes. In-Wheel Motor (Hub motor) can be used in electric cars with 4 wheel independent drive configuration. Within every wheel, there can be one "Direct-Drive In-Wheel Motor" to generate the necessary torque per wheel. Unlike conventional "central drive unit" systems, torque as well as the power and speed can be supplied to each tire independently. The difference in this work is the design of a direct drive electric motor which is able to carry transverse loading acts on a tire. Type of the motor is called inverted configuration or outer rotor structure in the literature. The electric machine designed in this work is Switched Reluctance Machine. First a 3D solid model was created. Necessary strength analyses have been done. Simultaneously, electromagnetic FEA has been done, when it is necessary either of the designs were modified until it converged to a set of consistent dimensions for both mechanic and electromagnetic design. Last, the results of the electromagnetic analysis were embedded into a hybrid simulation model, in order to check the coherency between the design and the analysis. The results were coherent.**

I. INTRODUCTION

Theories about differential drive and skid steering go back in the history almost as long as the electric vehicle itself. The Lunar Rover Vehicle [1] was actually an independent drive configuration, with in-wheel motors.

Today the examples have multiplied. Many private companies are working on in-wheel motors. Most of the race-wining solar cars use this technology.

Having a fast torque response, electric motors are far better controllable then IC engines. If they are fitted inside the wheel of the vehicle, then many things change in today's world of cars.

Having a direct drive electric motor inside each wheel eliminates many of the conventional modules in the car; gearbox, differential box, drive shaft, and IC engine of course.

GM Hy-wire concept utilizes in-wheel motors. In this prototype everything that has anything to do with pushing the car is fitted inside the lower deck of the vehicle. This leaves a very large unused empty space ready to be re-utilized.

Having the driving torque directly on the road by eliminating all the gearbox and transmission, power loss is decreased quite a big amount. Moreover, regenerative breaking can be utilized more efficiently, since each wheel can be commanded independently. This concept also adds to the safety of the vehicle since all of those assistive technologies mentioned above can be realized in one unit, the electric motor itself. Since it has the ability to generate negative torque, it has a natural ABS ability along with the others.

II. SRM

Although the concept of the SRM (VRM) has been around for a long time, only recently have these machines begun to see widespread use in engineering applications. This is due in large part to the fact that although they are simple in construction, they are somewhat complicated to control. For example, the position of the rotor must be known in order to properly energize the phase windings to produce torque. It is only recently that the widespread availability and low cost of micro and power electronics have brought the cost of the sensing and control required to successfully operate VRM drive systems down to a level where these systems can be competitive with systems based on dc and induction-motor technologies [2]

In a simple SRM the coil inductance L varies with rotor position θ. Assuming that the rotor carries a constant current positive motoring torque is produced only while the inductance is increasing, and that happens as the rotor approaches the aligned position [3]. Passing the aligned position and entering a decreasing inductance profile, the attractive force between the poles produces a negative torque. If the machine rotates with a constant current in the coil, the negative and the positive torque impulses cancel, and therefore the average over a complete cycle is zero. To eliminate the negative torque impulses, the current must be switched off before entering the decreasing inductance zone. The ideal current waveform is therefore a series of pulses synchronized with the rising intervals.

Linear analysis assumes that the inductance is independent of current (in fact they are dependent): that there is no magnetic saturation. See Figure 11

Generally mutual coupling between phases is normally zero or small, and is ignored [3]. The voltage equation for one phase is [4]

$$v = Ri + \frac{d\psi}{dt} = Ri + \omega_n \frac{d\psi}{d\theta} = Ri + L\frac{di}{dt} + \omega_n i \frac{dL}{d\theta} \quad (1)$$

where v is the terminal voltage, i is the current, ψ is the flux-linkage in volt-seconds, R is the phase resistance, L is the phase inductance, θ is the rotor position, and w_n is the angular velocity in rad/s.

The instantaneous electric power is [4]

$$vi = Ri^2 + Li\frac{di}{dt} = Ri + \omega_n i^2 \frac{dL}{d\theta} \quad (2)$$

The rate of change in magnetic energy stored is

$$\frac{d}{dt}\left(\frac{1}{2}Li^2\right) = \frac{1}{2}i^2\omega_n\frac{dL}{d\theta} + Li\frac{di}{dt} \quad (3)$$

The mechanical power conversion $P = \omega_n T_e$ is what is after resistive loss and magnetic stored energy is eliminated from instantaneous power. Then the torque is

$$T_e = \frac{1}{2} i^2 \frac{dL}{d\theta} \qquad (4)$$

Notice that the torque is proportional to the square of the phase currents and that as a result it depends on only the magnitude of the phase currents and not on their direction.

Those linear approaches are valid only to a certain value that the linearity between flux-linkage and current cease to exist. In this situation the torque can be calculated via [5]

$$T_e = \frac{\partial W_c}{\partial \theta} \qquad (5)$$

where W_c is the co-energy which is defined as in Figure 1
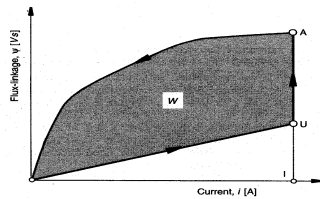
Figure 1. Co-energy

III. PROBLEM DESCRIPTION

A. Physical Constraints

The motor in the focus of this material is in-wheel motor. Therefore, its overall dimensions are limited with the empty space available inside the wheel. The cross-sectional view of a standard wheel in Figure 2 may give a pretty good idea about the problem.

a)   b)
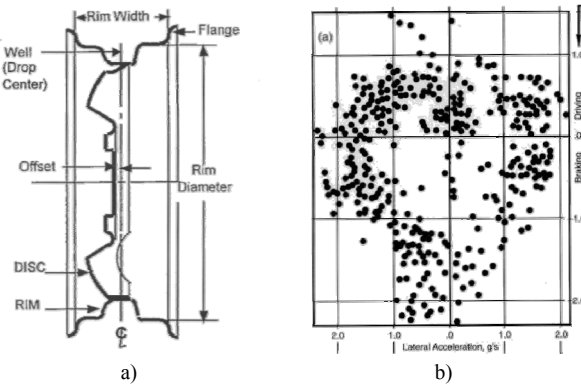
Figure 2. a)Sectional view of a wheel b)gg data of a grand prix car

Diameter-wise, because of the gnarled and wavy profile of the cross-section, generally for most of the wheel types only 80% of the diameter is available for insertion.

For class-A, light weight cars, generally R13 and R14 size wheels are used by the manufacturers. Therefore the outer diameter of the designed motor will be taken as 290mm.

Width of the available space inside the wheel is another parameter that affects the torque output, and driving characteristics of the vehicle also. In the end, it is decided that the shaft length will not exceed 160mm.

B. Mechanical Constraints

The motor must be able to withstand the every force that may act on a tire. The magnitude of total traction a tire can supply is limited and is a function of vertical loading, road surface, and contact patch profile. This traction is shared between lateral and longitudinal tractions. If one of them, say longitudinal (such as in hard braking) uses up all the available traction, then since there is no lateral traction available the vehicle starts to skid towards the sides. This property is often visualized as a traction circle, but actually it is an offset ellipse.

Figure 2.b shows the data captured in a grand prix car. On the figure traction circle can be clearly seen. The data in the figure reads that for forward acceleration the traction value is upper bounded with 1g, whereas for braking this climbs up to 2g. Again for the cornering limits traction can be taken up to 2g also.

Another important data source can be the data supplied by a major sensor company, Kistler [6-7]. The data supplied by the company belongs to a Class C car (mid-size) can be very useful to have an idea about the forces acting on a tire.
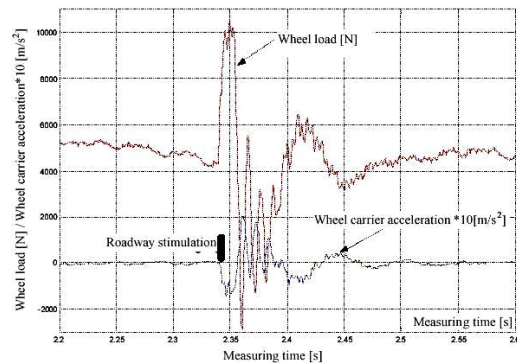
Figure 3. Wheel load data (Kistler's Data) [6]

This data shows that on a bumpy road the vertical loads may climb up to 10000N. Also due to weight transfer for a 1250kg car during a sharp cornering, the vertical load can easily climb 50% of the vehicle's weight, which is around 6000N. And if the road conditions are added to this number, to design the shaft for a vertical load of 12000N seems quite reasonable and safe. (Safety factor=2)

There are also impact conditions but they are handled different than static analysis.
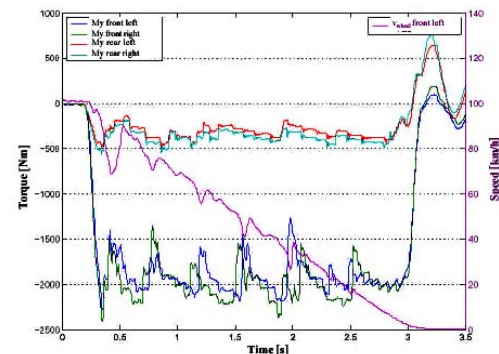
Figure 4. Braking force distribution on ABS regulating process [7]

Yet again, that is not all. Another thing that needs to be handled is the moments that may be acting on the tire. Figure 4 shows the moments acting in an ABS assisted braking.

The maximum moment is around 2200Nm. Since lateral forces are bounded by the maximum traction available, again that moment can not exceed 2200Nm.

As a result, design values for braking and cornering is taken as 3000Nm.

C. *Electromechanical Constraints (Torque Demand)*

There exist many resistive forces acting on a vehicle on the move. These are rolling friction, aerodynamic drag force, and internal frictional resistance in moving parts such as gear boxes, differentials, and bearings. In this document only first two will be taken into account to calculate the necessary power to be developed per motor.

Rolling friction depends on both tire and road surface characteristics, namely the interaction between these two. However, since the tires in focus of this material are conventional types, it can be said that it depends on the road type.

Using 3 different rolling friction values together with some appropriate tire dimensions and vehicle mass, it is quite straightforward to calculate necessary torque and power as a function of road surface conditions and vehicle speed. A matlab script was written for this purpose and the output comes out as the following figure.
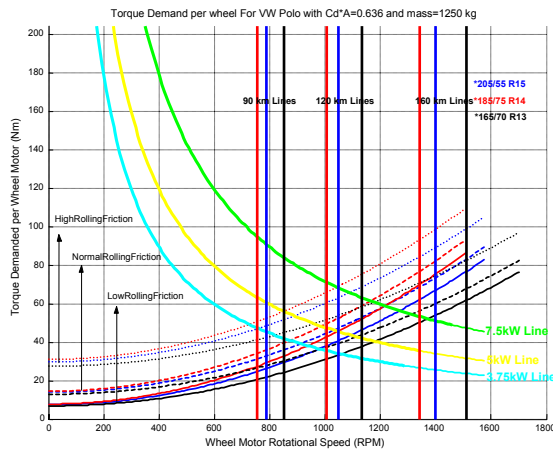
Figure 5. Power & Torque demand per wheel

Looking at the Figure 5, one can easily state that under normal rolling friction conditions and using 185/75 R14 type tires, 2.5kW per wheel will be enough to reach a top speed around 90 km/h on a flat road. That also means that the in-wheel SRM has to be able to give a torque output of at least 35Nm at 800 rpm. The reason why 90km/h is selected as a target speed is that it's top legal speed in most of the countries all around the world.

IV. DESIGN PROCESS

A. *Mechanical Design*

Generally hub design is one of the most critical parts of the vehicles. They must withstand all the load conditions a vehicle can undergo. In this case it was the same. The proposed design can be seen in Figure 6.b

The loading condition considered is combination of vertical loading, cornering force plus produced torque depending on the longitudinal traction available at the moment.

Figure 6. Loading Condition; a) A cornering b) Loading on the shaft

Considering the torque versus rotational speed characteristic of the SRM, and with more current boosting for a short time, it's reasonable to think about a maximum brake torque of 110Nm.

This value was reflected as distributed forces acting on the groove walls in the FEA.
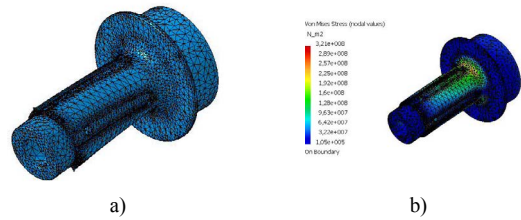
Figure 7. FEA Results; a) Mesh Structure, b) Von Misses Stresses

Looking at the results it can be clearly seen that the neck region is still dominating by means of stress concentration. Maximum Von Misses stress is 328 MPa and this occurs around the neck not on the groove corners. This magnitude of torque is quite harmless for the design since the yielding stress of carbon steels can be between 200-600 MPa.

B. *Electromagnetics*

Here comes the most important part; the power developed out of this machine:

$$P_d = k_e k_d V i m \qquad (6)$$

k_e is the efficiency, it will be taken as 0.85 in this calculation, and k_d is the duty cycle which can be expressed as;

$$k_d = \frac{\theta_i q P_r}{360} \qquad (7)$$

Combining these, the power developed can be rearranged to give [4]

$$P_d = k_e k_d k_1 k_2 B A_s D^2 L N_r \qquad (8)$$

Here $k_1 = \pi^2/120$. Parameter k_2 is related to the different characteristic inductances of the machine. The literature says that in general this parameter can be bounded as the following $0.65 < k_2 < 0.75$ [4,8]; In this case it is taken as 0.65.

A_s is called the specific electric loading [4];

$$A_s = \frac{2 T_{ph} i m}{\pi D} \qquad (9)$$

Here *m* stands for the number of phases conducting at the same time, which in this work is always 1. Again for A_s it is stated that it is usually in the range of $25000 < A_s < 90000$ [4,8]. In this work, for the space

available inside the motor, a low value of A_s fits better. It is simply a question of how many number of turns you can fit inside for a specific design current. Then a value of 24000 is found the best.

The duty cycle k_d can be taken 1, since the current conduction angle θ_i is supposed to be maximum 15° for 6/8 machine. Then another parameter comes on the scene, and that is stroke angle ε [3];

$$\varepsilon = \frac{2\pi}{qP_r} \qquad (10)$$

where $q = Ps/2$. In this case ε is 15°.

This may lead the discussion into a new conclusion. Since for a SR machine with its rotor and stator pole numbers are known, its stroke angle is fixed also. This stroke can be applied only during increased inductance and that puts a lower bound on the stator arc dimension as the following;

$$\min[\beta_s] = \frac{2\pi}{\frac{P_s}{2}P_r} \qquad (11)$$

In this design of SRM with a 6/8 configuration $\min[\beta_s] = 15^o$. Now it is necessary to come up with a number for β_s. Publications on this matter [9] are generally concentrated on a ratio called '*Stator Pole Enclosure*'. It is defined as the ratio of β_s to the pole gap, which is the angle between two successive poles. Then;

$$\beta_s = \frac{2\pi}{P_s} StatorPoleEnclosure \qquad (12)$$

Table 1. Motor's Data

Number of Stator Poles	6
Number of Rotor Poles	8
Stator Pole arc β_s	18°
Rotor Pole arc β_r	22°
Air-gap thickness l_g	0.4 mm
Stack length L	50 mm
Bore diameter D	200 mm
Shaft diameter D_s	45 mm
Rotor outer diameter	290 mm
Back-iron thickness	22mm
Turn/phase	120
Coil wire dimension	9 AWG
Base current	45 A
Lamination material	M19 steel
Phase resistance	0.06 Ω
Copper Loss (@base current)	120 W
Average torque (900 rpm)	33 Nm
Continuous Power	3.2kW
Peak Power	9 kW
Insulation Class	B

Although Krishnan's empirical results [9] claim that generally the best values lie between 0.35-0.45, a value of 0.30 was decided. Then β_s becomes 18°.

Having decided the values of β_s, A_s, and k_2, D can be calculated using (8). Accordingly then, stator pole thickness, Back-iron thickness for stator b_{sy} and rotor b_{ry},

stator h_s and rotor pole heights h_r, rotor pole arc β_r, fall-angle θ_{fr}, fall-time T_f can be calculated using standard procedure discussed in [4];

Then comes the stator phase resistance and Turn/phase calculations. Having calculated those according to the geometry of the machine dimensions below are calculated.

Having completed the dimensioning, the next step is to make the necessary simulations and the analysis for this new designed machine. In order to overcome nonlinear nature and analytical solution problems, numerical methods and finite element tools are utilized.
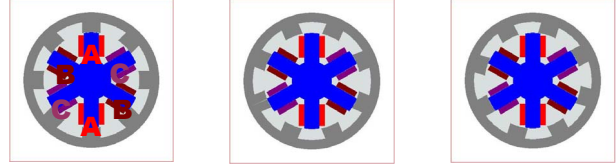
Figure 8. SRM's three distinctive rotor positions for PhaseA; (left) Aligned, (middle) Unaligned, (right)Aligning just begins

Designed motor is 6/8 type, which means it has 8 rotor poles, and 6 stator poles. Since base current was designed as 45A, it is necessary to make sure that the parametric solution covers at least two times of this value for all phases. In this case, it means 90A.

In Figure 9 reader can see an example mesh used in Maxwell2D. That structure consists of around 8000 triangles and the more than half of these triangles are in the thin air-gap. That is because the air-gap plays a major role in the torque production. In the electromagnetic conversion most of the energy is stored within this thin band.
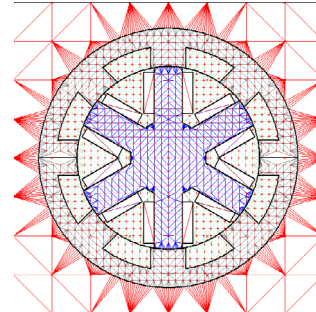
Figure 9. Maxwell2D mesh for SRM model

Below in Figure 10 one of the results of the simulation can be seen. It is the flux distribution for aligned and just overlapping positions at 45 A with phase excitation.
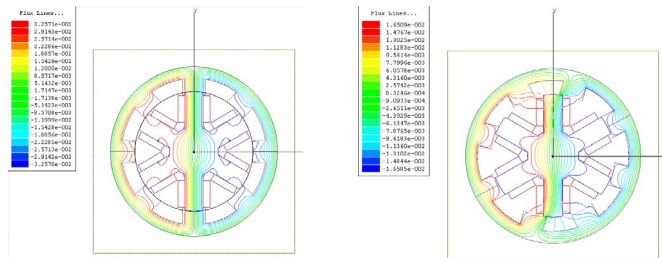
Figure 10. Flux line distribution with 45A phase A excitation; (left) Aligned, (right) Overlapping begins

The results are coherent with the theory, and show that torque production is possible. During aligning flux path just finds a narrow way through, and flows in. Since the

cross sectional area at the moment is small for the flux magnitude, B increases significantly in that zone. Another thing is that the maximum value of the B is given as 1.9 Tesla in the result. That shows that taking a value of 1.7 Tesla for B during the process of dimensioning was not that bad at all [4].

The next plots in this section have been generated by Matlab using the simulation outputs. First one is the flux linkage plot. There, it shows the flux linkage versus phase current A for different rotor positions between 0°-45°, namely the two aligned positions.
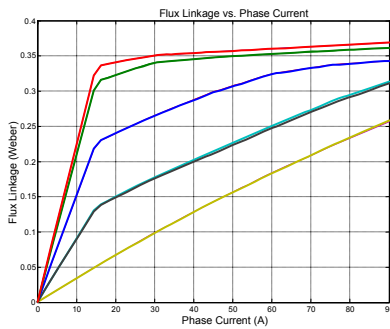
Figure 11. Flux Linkage vs. Current for phase A between 0°-45°

Saturation effect is quite obvious in the graph. After the current value of 15A medium starts to saturate and the inductance decreases significantly.

Torque generated is the most important result of all. After all, that is the main concern of this material. Figure 12 gives the results of the simulation for this concern.

It says that, at 45A it is possible get torque value of 35N, and at 90A it's able to supply a torque of 70Nm. It's also clear that for two positions, aligned and unaligned, torque production is 0 Nm.
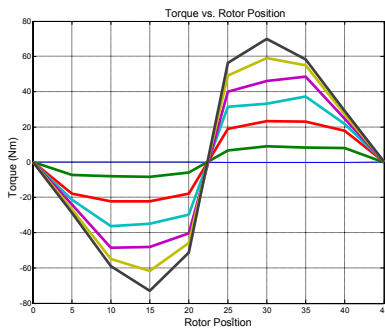
Figure 12. Torque vs. Rotor Position for currents 0-90 A
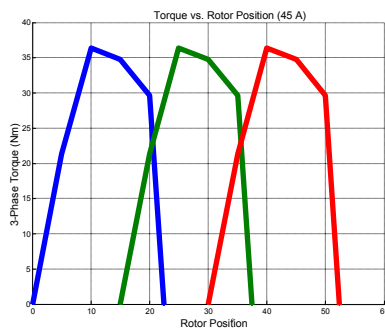
Figure 13. Continuous torque production (45 A)

The general appearance of the graph may look quite like what the theory says. However, there is one thing that may not be comforting; there is no constant torque region at all.

It is possible to see the continuous torque production in Figure 13. Continuous torque production is achieved by exciting all three phases with a phase difference. That phase difference is given by ε the stroke angle. In this case it is 15°. That magic moment, when one phase is shut down and the next one must be turned on, can be measured from the graph. It's around 22°

Another output of this simulation is the Torque-Current-Angle surface (Figure 14). This surface shows the torque as a function of current, and rotor position. Cutting this surface with various torque planes gives the Torque Contour graph (Figure 15). These two data can be valuable in order to see the capabilities of the motor.
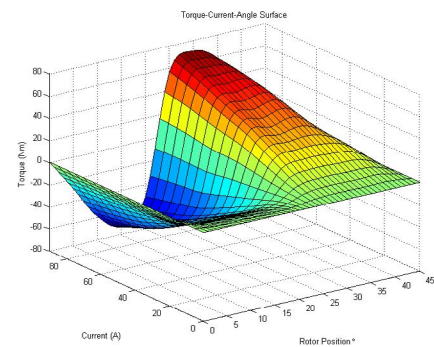
Figure 14. Torque-Current-Rotor Position surface
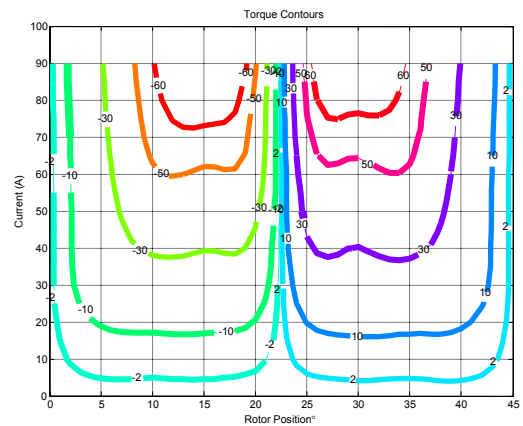
Figure 15. Torque contours for various torque values

Simulation results of the previous section shows many useful information. However, they are the product of Maxwell2D magnetostatic solver. Generally it is required to know transient behavior of the motor, so that one can observe the current, derivative of the current, back-emf, and voltage profiles during the operation.

A simulink model was prepared for this purpose. The main idea behind is sort of 'unique '. System does not use a full analytical solution, but instead it uses the benefits of the FEA solution that has been created by the Maxwell magnetostatic solver. In a way, it can be called a hybrid model.

Doing the simulations with a current controller driving a current 45A in trapezoidal profile the following results are obtained:
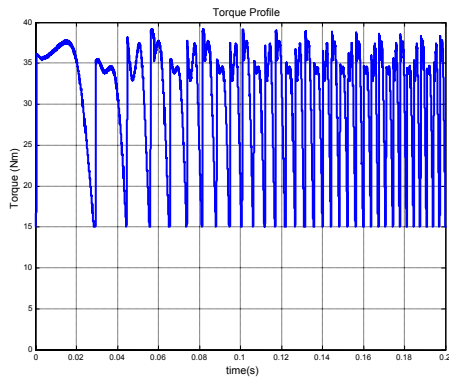
Figure 16. Torque Profile

Torque results reveal the amount of ripple. It is more than 50%. However the maximum torque is around 35Nm and the average can be found as 32Nm. These are coherent with the Maxwell results. The effect of ripple on the vehicles velocity can be seen in Figure 17. It has actually no effect because of the high equivalent inertia of the car.

Below performance speeding performance of a 1250 kg vehicle can be found. The torque reference for this test has be shaped so that for first 30 seconds the current will be tripled and after the phase is over it will drop the double for 10 seconds and in the end it will reach the base current.
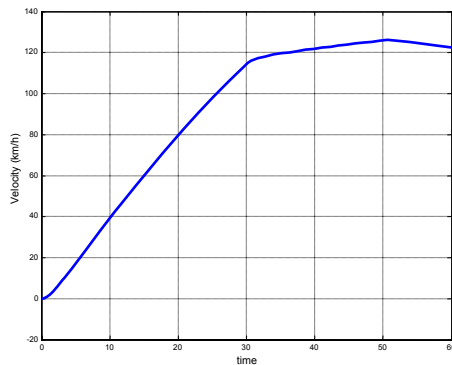
Figure 17. Speeding curve of a hypothetical vehicle

C. Heat Transfer

No detailed heat transfer analysis has been applied for the design. Instead, standard rules of National Electric Code of National Electrical Manufacturers Association (2001) were followed. In the end diameter, isolation coating thicknesses, and the current capacity (ampacity) of the magnet-wire was known. Accordingly, magnet-wire of 9AWG has chosen with heavy insulation and 62.5A ampacity (at 40°C)

V.   CONCLUSION

In this work an experimental in-wheel motor prototype has been designed. The necessity emerged from a plan to work on electric vehicle's control with 4-wheel independent drive configuration. Since it is much easier to use an already existing infrastructure, the proposed design had to be compatible with the class A cars on the market. The final product perfectly fits into a standard R14 wheel, and can be easily mounted to the knuckle of every class A-C car on the roads today. In addition the prototype will be able withstand the forces that were foreseen during the design. This means that with a proper control scheme, everything is ready to test it on the road.

The prototype's power can be argued to be its minus. Results of the simulink simulation show that it accelerates slower than a mediocre commercial IC engine vehicle. However, that performance criterion was never part of the design. Even it was, it might not be solved, at least with this configuration of SRM. A careful eye would catch it; the torque production zone, the laminations' stack thickness id only a 33% of the available space inside the wheel. In order to boost the design into a more dexterous machine, that problem has to be solved.

During the experimentation many aspects which were deliberately ignored in this thesis can be observed and considered as a data for the next design iteration. These are: Dynamic mechanical analysis, acoustic noise level of the motor, effect of variation of air-gap thickness due to forces acting on the tire and performance change of motor due to heat dissipation issues.

In the end, motor was designed and the simulations tell that the design specifications and the outputs are coherent and comparable.

REFERENCES

[1] Baker, David, Lunar Roving Vehicle: Design Report, *Spaceflight,* 13, 234-240, July 1971

[2] Fitzgerald. A.E., Jr. Kingsley. C, Umans. S. D., "Electric Machinery", Mc Graw Hill, 1992

[3] Miller. T.J.E., "Electronic Control of Switched reluctance machines", Newnes Power Engineering Series, 2001

[4] Krishnan. R., "Switched Reluctance Motor Drives", CRC Press, 2001

[5] Miller, T.J.E. and M. McGilp, "Nonlinear theory of the switched reluctance motor for computer-aided design", *IEEE Proc. B*, 137(6),337-346,1990

[6] Evers, W., Reichel, J., Eisenkolb, R., Enhart, I., "The wheel dynamometer as a tool for chassis development", Kistler Instrumente AG, SD920-234e,2002

[7] Amman, M., Evers, W., Streilein, V., "RoaDyn™-a development Tool for Braking Systems", Kistler Instrumente AG, SD920-234e,2002

[8] Radun, A.V., "Design considerations for switched reluctance motor", *IEEE Trans. On Industry Appl.*, 31, 1049-1087, 1995

[9] Arumugam, R., J.F. Lindsay, and R. Krishnan, "Sensitivity pole arc/pole pitch ratio on switched reluctance motor performance", IEEE Ind. Appl. Soc. Ann. Mtg. Conf. Rec., Oct. 1988, Pitsburg, PA, pp. 50-54